Thermochimica Acta, 125 (1988) 59–78
Elsevier Science Publishers B.V., Amsterdam – Printed in The Netherlands

STUDY OF AN ORDER–DISORDER TRANSITION BY DIFFERENTIAL SCANNING CALORIMETRY

M. HARMELIN, S. LEFEBVRE, M. BESSIÈRE and Y. CALVAYRAC

CNRS, Centre d'Etudes de Chimie Métallurgique, 15, rue Georges Urbain, 94407 Vitry-sur-Seine Cedex (France)

(Received 26 May 1987)

ABSTRACT

The DSC technique was tested for investigating order–disorder transitions in cristalline solid solutions. $Au_{75}Cu_{25}$ and $Au_{70}Cu_{30}$ alloys were taken as examples. The use of DSC in the isothermal mode only provides an insight into the rates of ordering near the critical transition temperature T_c, and does not allow an accurate determination of T_c and of the energy released during ordering. On the other hand, quantitative results can be obtained on continuous heating of the pre-annealed samples. The changes in enthalpy between different states of order were determined, and from these measurements kinetics of long-range ordering (LRO) and short-range ordering (SRO) were obtained. The change in the equilibrium value of the LRO parameter was studied with respect to temperature.

INTRODUCTION

Clear evidence of tiny structural modifications in alloys is often given by calorimetry. For instance, regarding amorphous metallic alloys, differential scanning calorimetry (DSC) [1,2] and electrical resistivity [3] are the only techniques which detect with a high sensitivity the structural changes attributed to variations of topological and compositional short-range order in the annealed amorphous alloys. Using direct methods of structural investigation, the structural changes involved were hardly detected. For example EXAFS and X-ray small-angle scattering did not detect any structural evolution [4], and a very carefully conducted neutron scattering experiment showed slight changes which did not lead to any detectable variation in either the number or the distance of first-neighbours pairs [5].

In crystalline solid solutions, order–disorder transitions result in large changes in the atomic arrangements. These changes are well measured by X-ray diffraction and by X-ray diffuse scattering. On the other hand, notwithstanding its high sensitivity, the DSC technique was scarcely used to study this type of transition [6]. The aim of this paper is to discuss the capabilities and limitations of DSC in determining the characteristic features

0040-6031/88/$03.50

of the long-range-ordering (LRO) and short-range-ordering (SRO) processes, i.e. the critical transition temperature T_c, the heat involved during ordering or disordering processes, and the kinetics of long-range and short-range ordering. For this investigation, the gold–copper system near $Au_{75}Cu_{25}$ was chosen. The existence of LRO in $Au_{75}Cu_{25}$ has been shown by Batterman [7] using X-ray diffraction. The ordering behaviour of this alloy has been studied by means of electron microscopy [8–10] and by measurement of electrical resistivity [11–16], of the Zener effect [17] and of shear-modulus [18]. The present DSC study is devoted to two alloys ($Au_{70}Cu_{30}$ and $Au_{75}Cu_{25}$) that we have previously studied by X-ray diffuse scattering [19–21] and by electrical resistivity [22]. Results are compared with the previous dynamic [6,11], isothermal [23] and solution [24] calorimetric studies.

Structural state

The Au-rich part of the phase diagram (around $Au_{75}Cu_{25}$) is shown in Fig. 1 which is taken from ref. 9. The low temperature phase ($L1_2$-type structure) is denoted structure **I**. At higher temperatures another phase appears (structure **II**), which is a one-dimensional periodical antiphase (PAP) superlattice. The order–disorder transition temperatures (T_c) have been measured by Batterman [7], Hirabayashi [16] and Davies and Funes [25]. The various temperatures obtained for different compositions are shown in Table 1.

The phase transformations, which take place at low temperatures, are very sluggish for compositions close to $Au_{75}Cu_{25}$. The nature of the ordered phase below T_c has been elucidated by electron microscopy using samples

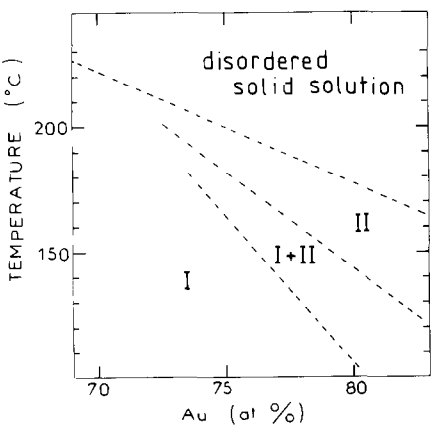

Fig. 1. Schematic phase diagram of the Au–Cu system in the Au-rich part: **I**, $L1_2$ structure type; **II**, one-dimensional periodical antiphase superlattice (from ref. 9, with permission).

TABLE 1

The order–disorder critical transition temperature (T_c) of Au–Cu alloys as determined by several techniques in the range of compositions between 68 and 75 at% Au

Au content (at%)	T_c (°C)	Technique	Reference
68	231 ± 3	X-ray	7
70	221 ± 2	X-ray	7
72	209 ± 2	X-ray	7
72.5	212 ± 1	Calorimetry	23
75	199 ± 3	X-ray	7
75	204		30
75	207	QDTA	6

quenched from a temperature close to the melting point ($T_m - 20°$) in order to increase the concentration of vacancies and, consequently, the rate of ordering and the size of the antiphase domains. Structure **II** appears for all compositions between 70 and 75 at% Au [9,20].

Definitions

In order to specify the degree of order, the arrangement of the atoms on the lattice sites is described by two parameters:

(i) the S parameter, in the long-range-ordered state (LRO) was introduced by Bragg and Williams [26]; it measures the tendency for each species of atom to be on a given sublattice. For $Au_{75}Cu_{25}$ there are four simple cubic sublattices and, for perfect order, one is occupied by Cu ("β sites") and the other three by Au ("α sites"). If c_A and x_A are respectively the atomic fraction of Au atoms in the alloy and the fraction of Au atoms on α sites, the S parameter is defined by the ratio

$$S = \frac{X_A - c_A}{1 - c_A}$$

For a stoichiometric $Au_{75}Cu_{25}$ alloy with perfect order, $S = 1$. For the non-stoichiometric alloy $Au_{70}Cu_{30}$ the maximum value of S is

$$\frac{c_A}{3(1 - c_A)} = 0.78$$

S decreases slowly with increasing temperature, until it drops discontinuously to zero at T_c.

(ii) the α parameter defines the state of short-range order. Above T_c there is no long-range order. However, there is a preference in the kind of close neighbours around each atom. This departure from randomness is described

by the Warren-Cowley α parameter [32] which is defined for the atomic site with coordinates l, m, n with respect to a given A atom as

$$\alpha_{lmn} = 1 - \frac{P_{lmn}}{c_B}$$

where P_{lmn} is the probability that the atomic site is ocupied by a B atom.

EXPERIMENTAL

Preparation of the samples

The $Au_{75}Cu_{25}$ and $Au_{70}Cu_{30}$ ingots were prepared from 99.999% Au and 99.999% Asarco copper by melting under vacuum (1×10^{-6} torr). The X-ray diffuse scattering study requires single crystals. They were grown by a horizontal Bridgman method. The DSC samples were cut off from these single crystals. The DSC samples were ~ 2 mm thick and ~ 5 mm in width. Short annealing treatments were performed in situ in the DSC cell (as described later). Long annealing treatments (> 65 h) were carried out in a sealed evacuated silica tube heated in a separate furnace.

DSC measurements

A Perkin–Elmer DSC-2C device connected to a 3500 thermal analysis data station was used for the calorimetric measurements. Sample weight was 980 mg for $Au_{75}Cu_{25}$ and 986 mg for $Au_{70}Cu_{30}$. Pure gold (1176 mg) was used as a reference. Thus, assuming an ideal solid-solution behaviour for $Au_{75}Cu_{25}$ and $Au_{70}Cu_{30}$, heat capacities of the sample and the reference were equilibrated within 2%. The sample and the reference were put in the DSC cell without its pan; the atmosphere was pure argon.

PRELIMINARY DSC TESTS

According to the simplified treatment proposed by Kessis [27] the equation of the base line may be written as

$$T_S - T_R = \Delta T = \beta\left(\frac{m_R C_{p_R}}{K_R} - \frac{m_S C_{p_S}}{K_S}\right) + \left(\beta\frac{m_S C_{p_S}}{K_S} + T_{0_S}\right)\exp\left(\frac{tK_S}{m_S C_{p_S}}\right) - \left(\beta\frac{m_R C_{p_R}}{K_R} + T_{0_R}\right)\exp\left(-\frac{tK_R}{m_R C_{p_R}}\right) \quad (1)$$

where S and R refer respectively to the sample and to the reference. T is the temperature, β is the heating rate, m is the specimen weight, C_p is the

specific heat, K is the superficial exchange coefficient between the specimen and the temperature sensor of the DSC detecting head, T_0 is the initial temperature, and t is the time.

Equation (1) shows that when an experiment starts and when no transition occurs the drift of the base line presents an initial thermal transient desequilibrium period corresponding to the two exponential terms: the higher the heating rate and the mismatch between the sample and the reference, the greater the thermal desequilibrium of the DSC cell.

Therefore, we have performed several preliminary tests in order to establish the best experimental conditions. Moreover, several isothermal experiments were carried out in order to check the ability of the DSC to follow the long-range- and short-range-ordering processes.

Isothermal tests

For these isothermal tests, the samples were first disordered at 350 °C and then rapidly cooled (320 °C min^{-1}) to the isothermal annealing temperature.

The result of an isothermal experiment performed with a specimen of $Au_{75}Cu_{25}$ is presented in Fig. 2 as an example of long-range ordering. The DSC curve corresponds to the heat evolution recorded at 170 °C vs. time. It is compared to the evolution of a pure gold specimen and of an empty cell. The steady state of the base line is obtained after ~ 2 min for the empty cell and after ~ 3 min for the gold specimens. In the case of $Au_{75}Cu_{25}$ an exothermic effect due to ordering is detected. However, an accurate determination of the heat effect cannot be made for two reasons: (i) the beginning of the ordering effect interferes with the transient desequilibrium

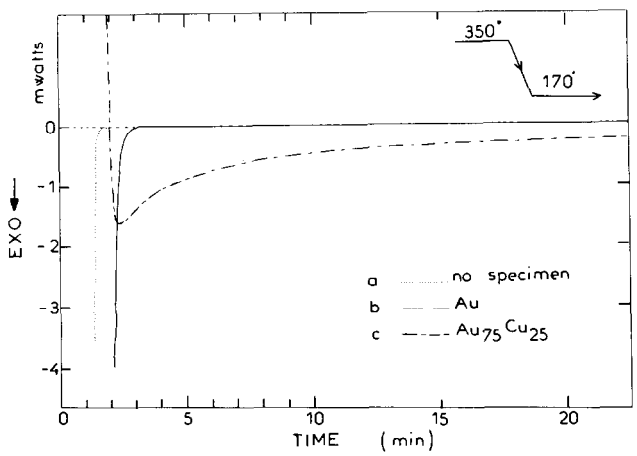

Fig. 2. Comparison of the DSC curves during an isothermal experiment (T_a = 170 °C) after cooling (at 320 °C min^{-1}) from 350 °C: a, no specimen in the DSC cell; b, gold specimens as sample and reference; c, $Au_{75}Cu_{25}$.

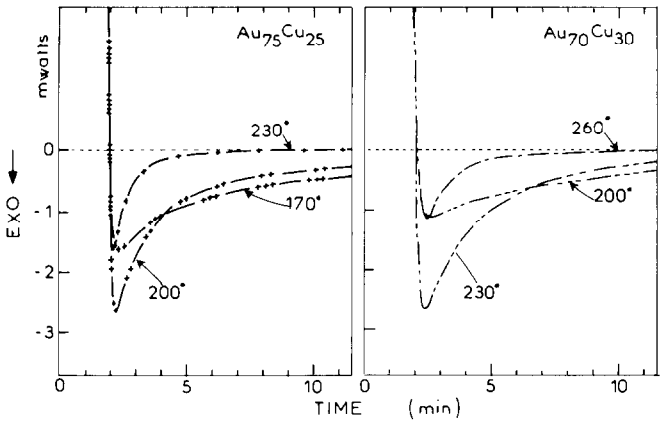

Fig. 3. A tentative determination of T_c by isothermal DSC tests on $Au_{75}Cu_{25}$ and $Au_{70}Cu_{30}$ cooled at 320 °C min^{-1} from 350 °C to T_a.

period and (ii) the ordering effect is too slow to be accurately followed until the completion of the process.

Regarding the determination of T_c, the isothermal tests performed on $Au_{75}Cu_{25}$ and $Au_{70}Cu_{30}$ are illustrated in Fig. 3. For both samples, the same kinetic behaviour is observed when the isothermal annealing temperature is increased from the LRO temperature range (e.g. 170 °C for $Au_{75}Cu_{25}$ and 200 °C for $Au_{70}Cu_{30}$) to the SRO range (e.g. 230 °C for $Au_{75}Cu_{25}$ and 260 °C for $Au_{70}Cu_{30}$). Around T_c, the short-range-ordering rate varies rapidly. At 230 °C for $Au_{75}Cu_{25}$ or 260 °C for $Au_{70}Cu_{30}$ the SRO attains its equilibrium value after annealing for 5 min. Below these temperatures, the short-range-ordering rate decreases. The DSC signal returns to the base line more and more slowly but the long-range-ordering rate is too slow for T_c to be accurately determined.

For these reasons, DSC experiments were not pursued in the isothermal mode. The ordering kinetics were not followed by direct DSC measurements. They were obtained by dynamic tests on disordering pre-annealed samples through T_c.

Dynamic tests

Influence of heating rate on the transient thermal effect

According to eqn. (1) the higher the heating rate, the greater the transient thermal desequilibrium on starting an experiment. A comparison of the transient desequilibrium effects obtained with different heating rates (1.25, 2.5 and 10 °C min^{-1}) is shown in Fig. 4. During these tests, gold specimens with identical weights (1186 mg) and nearly-identical shapes were used as sample and reference. In Fig. 4, T_i is the initial temperature of the run, T_e the temperature at which the steady state of the base line is attained. This

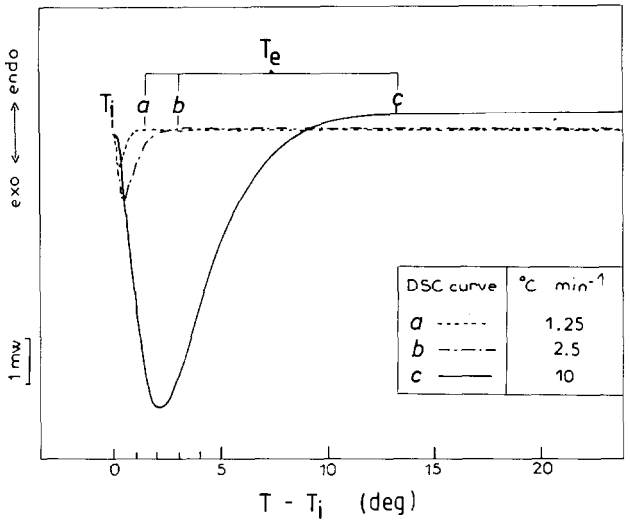

Fig. 4. Influence of heating rate on the transient thermal desequilibrium on starting a DSC experiment: T_i is the initial temperature of the run, T_e is temperature at which the steady state of the base line is attained.

figure clearly shows that the higher the heating rate, the stronger the initial transient thermal effect. The time interval between T_i and T_e remains practically the same (~ 90 s) for all heating rates. This leads to a temperature range ($T_e - T_i$) for the transient effect which is proportional to the heating rate. This "blind zone" is very detrimental for studying the disordering phenomena by DSC, especially for the enthalpy measurements.

A complete comparison of the transient period for heating rates increas-

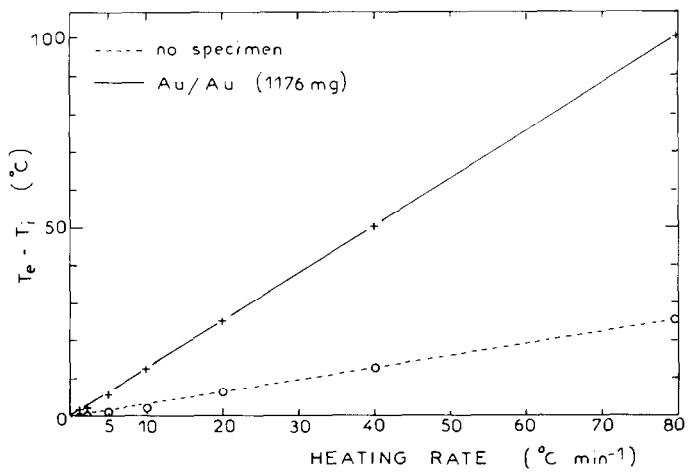

Fig. 5. Evolution of the transient thermal desequilibrium for heating rates increasing from 1.25 to 80 °C min^{-1} for an empty cell and for gold specimens as sample and reference.

ing from 1.25 to 80 °C min^{-1} is shown in Fig. 5. This figure also compares the magnitude of $T_e - T_i$ when the DSC cells are empty. From these results, it can be concluded that the lowest heating rate (1.25 °C min^{-1}) is the most appropriate for minimizing both the transient temperature interval and the amplitude of the parasitic transient heat effect.

Reliability of the enthalpy measurements on disordering

A sample of $Au_{75}Cu_{25}$ disordered at 350 °C was very rapidly cooled to 190 °C and annealed for 1 h at this temperature to obtain a long-range partially-ordered state. The sample was then heated either at 1.25 °C min^{-1} or at 10 °C min^{-1} starting directly from the annealing temperature. The corresponding DSC curves are shown in Fig. 6. In both cases an endothermic phenomenon is observed above the annealing temperature. Integrating the peak area for enthalpy measurements raises two difficulties: the beginning of the endothermic effect is lost because it is superimposed on the initial "blind zone" and the end of the phenomenon is difficult to determine on the high-temperature side. Three determinations were made as indicated in Fig. 6 for each heating rate; average values for ΔH of 180 ± 10 J mol^{-1} at 1.25 °C min^{-1} and 190 ± 10 J mol^{-1} at 10 °C min^{-1} were obtained. The accuracy of the ΔH measurements does not depend only on the heating rate ($\sim \pm 5\%$), but also on the choice of the final temperature limit for integrating the peak area ($\sim \pm 5\%$). Thus, a total error of $\sim \pm 10\%$ must be expected, with an additional error due to the loss of the heat effect during the "blind zone".

The influence of the heating rate is even more critical in the SRO range. Measurements of enthalpy changes are not reliable when the heating rate is

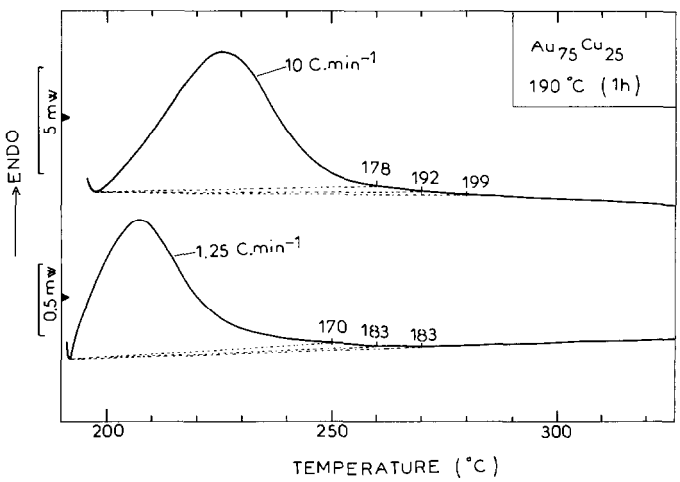

Fig. 6. Influence of heating rate and of the choice of T_e on the enthalpy measurement on disordering $Au_{75}Cu_{25}$ previously ordered for 1 h at 190 °C.

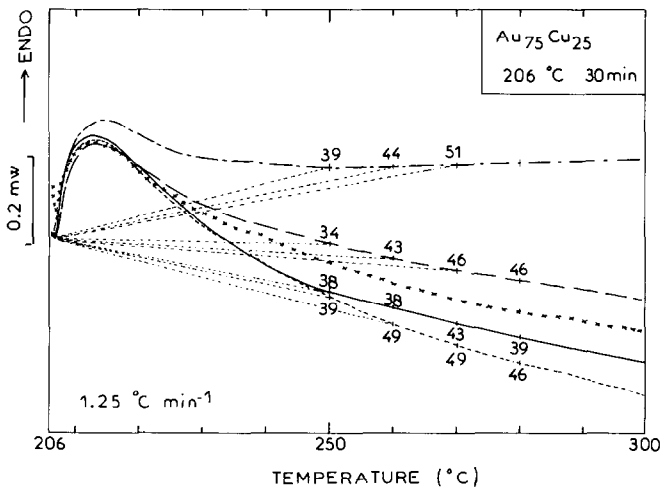

Fig. 7. Influence of the drift of the base line and of the choice of T_c on the enthalpy measurement on disordering $Au_{75}Cu_{25}$ previously ordered for 30 min at 206 °C.

greater than 1.25 °C min^{-1}. Another difficulty is the drift of the base line. Five similar experiments were performed with the same sample at different times (some months may separate the different experiments). The drift of the base line was not reproducible. Nevertheless, the measurements of the peak area within the temperature intervals indicated in Fig. 7 lead to an average value for enthalpy of 45 ± 5 J $(g\ at)^{-1}$.

Thus, it can be concluded that the error in the enthalpy measurements due to the variation of the heat transfer coefficients for different experiments is negligible compared with the error due to the choice of the temperature limits for integrating the peak area.

RESULTS AND DISCUSSION

We investigated the following characteristics of an order–disorder phase transformation:

(i) the heat effect corresponding to the disordering process or to a phase transformation in the ordered state;

(ii) the kinetics of the LRO process;

(iii) the change of the value of the equilibrium parameter S near T_c;

(iv) the kinetics of the SRO process.

Heat effect corresponding to the order–disorder reaction

As the LRO ordering process is very slow, $Au_{75}Cu_{25}$ and $Au_{70}Cu_{30}$ were annealed for several days at temperatures corresponding respectively to the

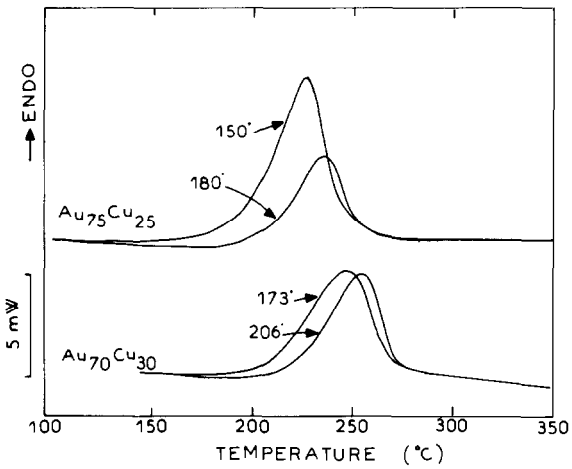

Fig. 8. DSC curves obtained on heating at 2.5 °C min^{-1} $Au_{75}Cu_{25}$ previously annealed at 150 and 180 °C, and $Au_{70}Cu_{30}$ previously annealed at 173 and 206 °C (cf. Table 2).

establishment of the $L1_2$ long-range order and of the periodical antiphase superlattice, i.e. at 150 and 180 °C for $Au_{75}Cu_{25}$ and at 173 and 206 °C for $Au_{70}Cu_{30}$.

For $Au_{75}Cu_{25}$ the corresponding DSC curves are shown in Fig. 8. After annealing at 150 °C, the enthalpy change from 150 to 300 °C is 1060 J (g at)$^{-1}$, i.e. twice the value measured after annealing at 180 °C [520 J (g at)$^{-1}$]. However, only one endothermic effect was always detected, without any splitting corresponding to the successive transformations. Furthermore, this endothermic effect always begins a few degrees above the annealing temperature. This may be explained by a decrease of the long-range-order parameter S with increasing temperature. Thus, the decrease of the enthalpy change after annealing at 150 or 180 °C is due both to the enthalpy of the transformation **I** → **II** and to the decrease of S.

For the non-stoichiometric composition $Au_{70}Cu_{30}$ the enthalpy changes corresponding to the two heat treatments are respectively 834 and 683 J (g at)$^{-1}$.

These values are compared in Table 2 with the other calorimetric determinations previously published in this range of composition. They agree with those obtained by Tissot and Dallenbach [6] by quantitative differential thermal analysis (QDTA) and by d'Heurle and Gordon [23] by isothermal calorimetry. These authors, who ignored the existence of PAP, have not studied the two transformations. Their annealing temperature and their calorimetric results show that the initial state of their alloys was a PAP structure. Using another technique (solution calorimetry) Deneuville [24] found a higher value. It seems that this discrepancy cannot be explained by a more-ordered state since the DSC kinetic investigations described below

TABLE 2

Enthalpy changes corresponding to the order–disorder reactions for various Au–Cu alloys annealed in the $L1_2$ and PAP range. Comparison of the DSC results with the other calorimetric determinations previously published

Au content (at%)	Annealing temp. (°C)	Annealing time (days)	Treatment [a]	Structure [19]	ΔH	
					Experimental [J (g at)$^{-1}$]	Calculated [28] [J (g at)$^{-1}$]
75	150	7	d	$L1_2$	1800 [24]	–
	150	7	c	$L1_2$	1060 [b]	1030
	180	7	c	PAP	520 [b]	670
	190	4	b,c	PAP	720 [6]	–
72.5	189	40	b	–	578 [23]	–
	194	40	b	–	573 [23]	–
	195.3	40	a	–	444 [23]	–
70	175	6	c	$L1_2$	637 [b]	–
	173	10	c	$L1_2$	834 [b]	934
	206	15	c	$L1_2$ + PAP	683 [b]	665

[a] a, b and c refer respectively to a sample which has been annealed above T_c and then: a, cooled directly to the ordering temperature; b, quenched to room temperature and subsequently reheated; or c, cooled directly to the ordering temperature then quenched to room temperature and reheated in the DSC cell. Sample d was annealed a few degrees below the melting temperature, quenched to room temperature and then annealed at 150 °C. [b] This work.

and the measurements of d'Heurle and Gordon show that the equilibrium state is attained with the annealing conditions we have used. It is possible that our DSC measurements give values systematically too low.

These thermodynamic results can be compared with the theoretical values calculated from the SRO parameters which were experimentally determined. In an Ising model limited to the configuration pair-wise interactions, energy is expressed as

$$E = \tfrac{1}{2}\Sigma\mu_i V_i \langle\sigma_i\rangle$$

where $\langle\sigma_i\rangle$ is the pair correlation function for the ith nearest-neighbour shell, μ_i the multiplicity of the pair i and V_i the pair-interaction potential.

For a binary alloy the pair correlation functions are directly related to the SRO parameters α_i measured by diffuse scattering experiments

$$\langle\sigma_i\rangle = 4C_A C_B(\alpha_i + 1) - 1$$

The pair interaction potentials may be calculated from the measured α_i, either through a thermodynamic approximation (cluster variation method, mean field approximation) or by a Monte-Carlo method. These pair-interaction potentials are defined by the change in energy when building an atomic pair AB of ith neighbours

$$V_i = \tfrac{1}{4}\left(V_i^{AA} + V_i^{BB} - 2V_i^{AB}\right)$$

TABLE 3

Values of the SRO parameters α_i measured at 300 °C [19–21] and of the pair-interaction potentials V_i calculated by a Monte-Carlo method [28]

i	lmn	α_i measured at 300 °C		V_i (meV) calculated	
		$Au_{75}Cu_{25}$	$Au_{70}Cu_{30}$	$Au_{75}Cu_{25}$	$Au_{70}Cu_{30}$
1	110	−0.071	−0.074	5.27	5.07
2	200	0.103	0.108	−3.31	−2.76
3	211	−0.027	−0.033	1.38	1.62
4	220	0.044	0.048	−0.33	−0.21

Taking into account four pair-interaction potentials, the configuration enthalpy is written

$$E = 6V_{110}\langle\sigma_{110}\rangle + 3V_{200}\langle\sigma_{200}\rangle + 12V_{211}\langle\sigma_{211}\rangle + 6V_{220}\langle\sigma_{220}\rangle$$

Assuming that there is no variation of these pair-potential interactions with temperature and neglecting the volume change, the change in energy between two known states of order can be calculated and compared with the enthalpy change measured by DSC. The values given in Table 3 have been obtained using a Monte-Carlo method [28]. Four pair-interaction potentials were calculated using the α_i parameters measured at 300 °C [19–21] far from the transition temperature ($T/T_c = 1.2$), where the calculation is more easy. Assuming no variation of these potentials with temperature, a Monte-Carlo calculation gives the pair correlation functions for the other states of order. The values of change in enthalpy obtained with this method are very close to those deduced from the DSC measurements (Table 2).

Kinetics of long-range ordering

In a Bragg Williams approximation and for a rigid Ising model which does not take into account lattice vibrations and static atomic displacements, the configuration energy is proportional to S^2. Thus the variation of $\sqrt{\Delta H}$ with time gives information on the long range ordering.

The experimental procedure used for the DSC experiments was the following: after disordering at 400 °C, the samples were ordered at a given temperature (T_a) for a given time (t_a). Then they were heated from T_a to 400 °C at 1.25 °C min^{-1}. Figure 9 shows typical DSC curves, obtained for $Au_{75}Cu_{25}$ after annealing at 190 °C for various times. The peak area increases with annealing time and the peak maximum is regularly shifted towards higher temperatures. Thus for $Au_{75}Cu_{25}$ the more developed the state of order (LRO parameter S and domain size), the higher the temperature of the maximum rate of destruction of order, that is the greater the resistance to the destruction of order. This behaviour is different from that of $Au_{70}Cu_{30}$: for this composition, all the DSC curves are gathered inside

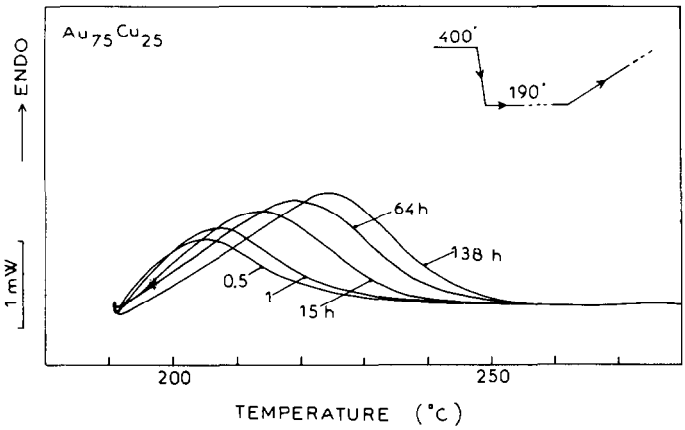

Fig. 9. Typical DSC curves obtained for $Au_{75}Cu_{25}$ after annealing at 190 °C for various times. Cooling rate from 400 to 190 °C, 320 °C min^{-1}; heating rate from 190 °C, 1.25 °C min^{-1}.

the same temperature interval (Fig. 10a). This difference is really typical of these compositions and does not depend on the DSC experimental conditions.

For $Au_{70}Cu_{30}$ for short annealing times (e.g. 15 min) an exothermic effect is detected between ~ 160–220 °C. This exothermic effect is enhanced when the disordered sample is cooled from 400 to 100 °C without stopping at 175 °C as is shown in Fig. 10b, an enlargement of Fig. 10a. This effect is the manifestation of short-range ordering during the scan.

The results of all the kinetic measurements are shown in Fig. 11 for both alloys. For $Au_{70}Cu_{30}$ the heat effects increase up to a steady value attained after about 250 h. The final value [637 J (g at)$^{-1}$] may be considered as corresponding to the establishment of the equilibrium LRO at 175 °C. This value is significantly different from that previously determined after annealing at 173 °C [834 J (g at)$^{-1}$]. As shown in Fig. 11, a small variation of the annealing temperature induces a large variation of ΔH, so that the absolute accuracy (a few degrees) in the determination of the annealing temperature may explain this discrepancy.

Is it possible to go further for a better understanding of the kinetics of long range ordering? For an infinite annealing time ($t_a = \infty$) the order parameter S_∞ attains its maximum value. For $t_a = 0$, $S = 0$. We can follow the evolution of the ratio

$$y = \frac{S_\infty - St_a}{S_\infty - S_0} = \frac{S_{max} - St_a}{S_{max}} = \frac{\sqrt{\Delta H_{max}} - \sqrt{\Delta Ht_a}}{\sqrt{\Delta H_{max}}}$$

The plot of log y vs. time is given in Fig. 12. For the same composition all the curves are well gathered but the kinetics are not simple. Two ordering

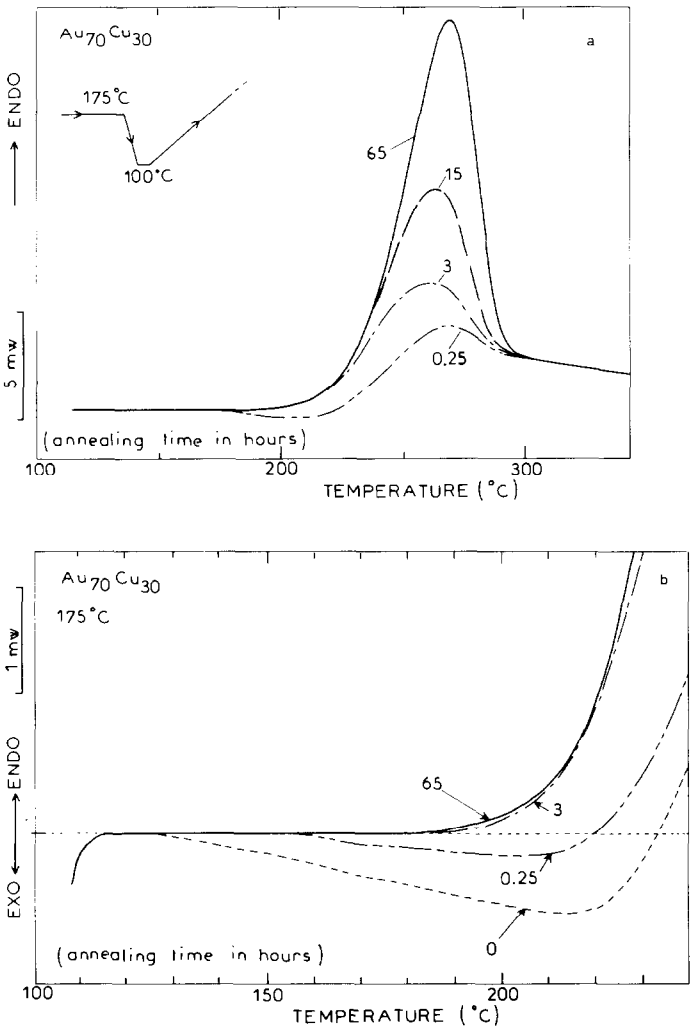

Fig. 10. Typical DSC curves obtained for $Au_{70}Cu_{30}$ after annealing at 175 °C for various times. Cooling rate from 175 to 100 °C, 320 °C min^{-1}; heating rate from 100 °C, 10 °C min^{-1}. Annealing time at 100 °C was 5 min for all samples.

stages occur: first, a rapid one and secondly a very slow one. This result is confirmed by resistivity experiments [22]. It may be expected that the first stage is due both to short-range ordering and nucleation of long-range ordering and the second one to the development of long-range ordering.

Variation of the LRO order parameter S with temperature ($Au_{75}Cu_{25}$)

A first-order transition is characterized by a discontinuity of the thermodynamic properties at T_c, and particularly by a discontinuity of S. This is

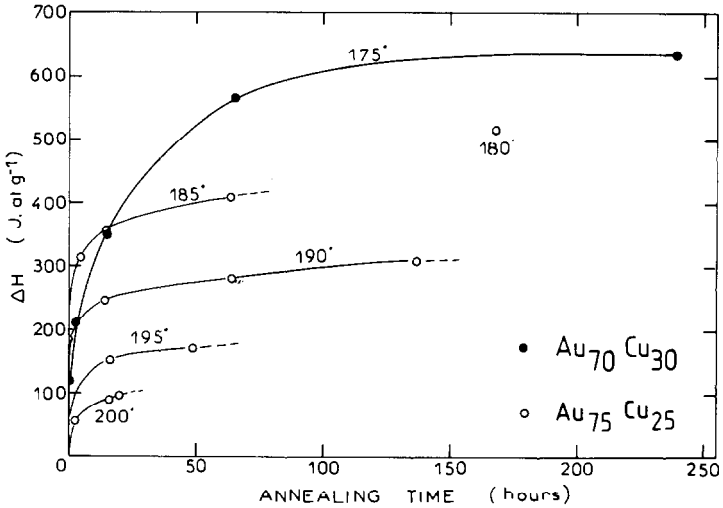

Fig. 11. Comparison between the kinetics of long-range ordering in $Au_{70}Cu_{30}$ and $Au_{75}Cu_{25}$.

very clearly demonstrated in the case of Cu_3Au where S (measured by X-ray diffraction) decreases slowly with increasing temperature from $\sim 100\,^{\circ}C$ below T_c and drops discontinuously at T_c [29].

In order to study equilibrium order vs. temperature, we made DSC measurements of the enthalpy change on disordering the $Au_{75}Cu_{25}$ sample pre-annealed for a long time at different temperatures below and above T_c. From these measurements the temperature dependence of the energy is shown in Fig. 13. The evolution is quite similar to that observed for

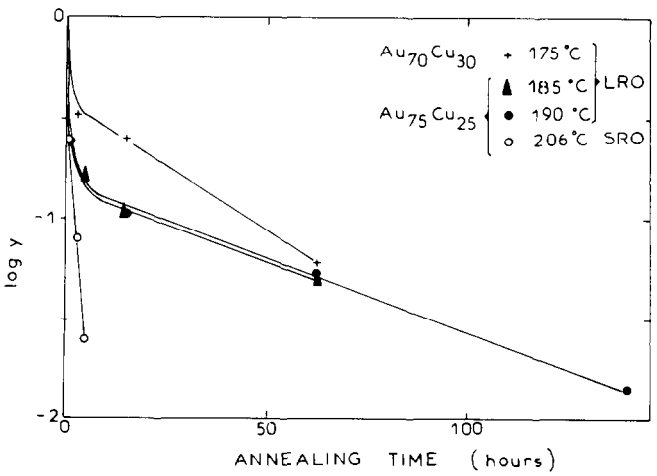

Fig. 12. Plot of $\log\ y = \log\ [(\sqrt{\Delta H_{max}} - \sqrt{\Delta H t_a})/\sqrt{\Delta H_{max}}]$ versus annealing time for $Au_{70}Cu_{30}$ ($T_a = 175\,^{\circ}C$) and for $Au_{75}Cu_{25}$ ($T_a = 185$, 190 and $206\,^{\circ}C$).

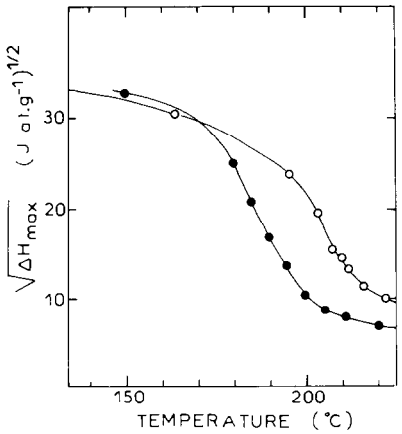

Fig. 13. Plot of $\sqrt{\Delta H_{max}}$ vs. annealing temperature for $Au_{75}Cu_{25}$ (●). Comparison with the results obtained by d'Heurle and Gordon [23] for $Au_{72.5}Cu_{27.5}$ (○). The order parameter S varies as $\sqrt{\Delta H_{max}}$.

$Au_{72.5}Cu_{27.5}$ by d'Heurle and Gordon [23], reported on the same figure. The curve does not present any discontinuity at T_c and is therefore quite different from the theoretical one. So, a question is raised: was equilibrium fully attained at the temperatures considered? An argument is provided by a "cross-experiment" (Fig. 14); a sample annealed for 15 h at 185 °C is rapidly heated to a higher temperature (190 °C): the energy decreases to the expected equilibrium value at 190 °C. Therefore the equilibrium order was attained at 190 °C, and we may assume that the curve in Fig. 13 describes

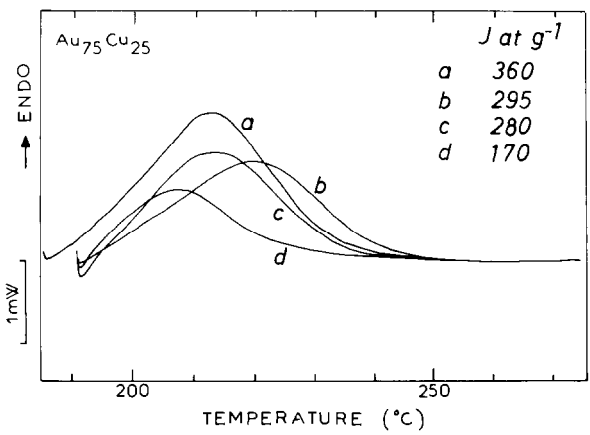

Fig. 14. DSC curves obtained on heating at 1.25 °C min^{-1} $Au_{75}Cu_{25}$ previously annealed at a, 185 °C for 15 h; b, 190 °C for 64 h; c, 185 °C for 15 h + 190 °C for 1 h; d, 190 °C for 1 h. Results of the enthalpy measurements corresponding to the respective DSC curves are given in J (g at)$^{-1}$.

the equilibrium order vs. the temperature. So the question still remains: why is no latent heat observed at T_c? The decrease in S with increasing temperature is nearly linear over a large interval of temperature (20 °C). This trend may be expected when passing through a two-phase region of ordered and disordered phases if the fraction of the disordered phase increases with increasing temperature. The existence of such a two-phase domain still remains to be proved.

Kinetics of short-range ordering

Typical DSC curves are shown in Fig. 15 for $Au_{70}Cu_{30}$ (at 230 °C) and in Fig. 16 for $Au_{75}Cu_{25}$ (at 206 °C). In both cases, samples were previously disordered at 400 °C inside the DSC cell and then quickly cooled to the annealing temperature T_a. Then the samples were heated starting from T_a. Figures 15 and 16 show the progressive increase in intensity of the DSC peaks with annealing time. For $Au_{70}Cu_{30}$ all the DSC curves are gathered inside the same temperature interval, as for long-range ordering (Fig. 10a). Stabilization was obtained after 5 h. For $Au_{75}Cu_{25}$ the peak temperature is regularly shifted towards higher temperatures. This behaviour is also similar to that observed for long-range ordering (Fig. 9) for this composition. The equilibrium is nearly attained after annealing for 15 h. This result agrees with those obtained from electrical resistivity measurements: at 205 °C the resistivity attains a plateau after annealing for 8.5 h [31].

A comparison between the respective kinetics is given in Fig. 17 for both compositions and for different temperatures: 206, 212, 218 and 230 °C for $Au_{75}Cu_{25}$ and 230 °C for $Au_{70}Cu_{30}$. Figure 17 clearly shows that the

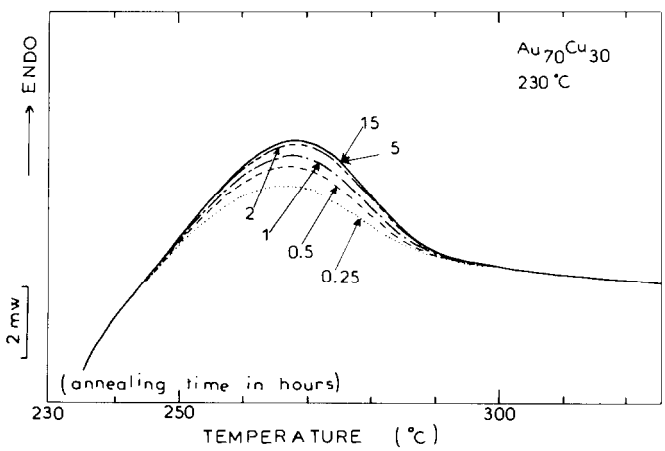

Fig. 15. DSC curves obtained on heating at 10 °C min^{-1} $Au_{70}Cu_{30}$ previously annealed at 230 °C for various times.

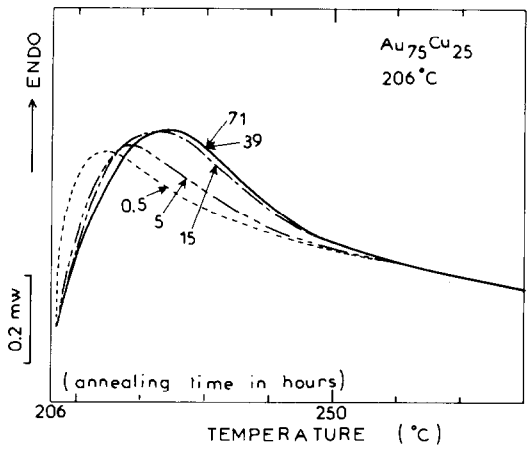

Fig. 16. DSC curves obtained on heating at 1.25 °C min^{-1} $Au_{75}Cu_{25}$ previously annealed at 206 °C for various times.

short-range-ordering rate in $Au_{70}Cu_{30}$ is faster than in $Au_{75}Cu_{25}$. The values we have measured for the change in configuration energy in $Au_{70}Cu_{30}$ and $Au_{75}Cu_{25}$ [Fig. 17: 145 and 120 J (g at)$^{-1}$, respectively] are slightly smaller than those obtained for the relaxation enthalpy of amorphous alloys. In the amorphous alloys that we have studied [2,4,5], two major effects were observed by means of DSC: (i) an exothermic (irreversible) phenomenon during the first heating of the as-quenched specimen generally attributed to changes in topological short-range order ($\sim$ 1–2 kJ mol^{-1}) and (ii) an endothermic phenomenon on heating the pre-annealed specimen in the glass

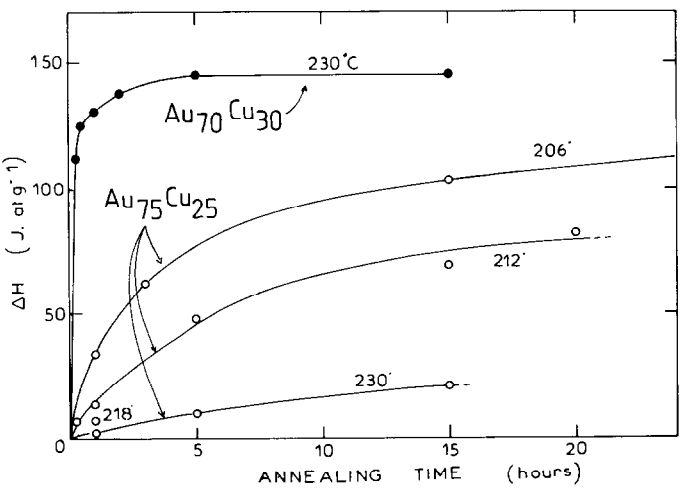

Fig. 17. Comparison between the kinetics of short-range ordering in $Au_{70}Cu_{30}$ and $Au_{75}Cu_{25}$.

transition range; the intensity of this latter effect was shown to be dependent on the decrease of the configuration enthalpy (ΔH_σ) during the annealing treatment. It is generally attributed to changes in chemical short-range order. The maximum value of ΔH_σ that we have found is ~ 800 J mol^{-1}.

CONCLUSIONS

From the above results on $Au_{75}Cu_{25}$ and $Au_{70}Cu_{30}$ it appears that DSC can provide valuable information about the order–disorder transition in cristalline solid solutions.

Isothermal tests give an insight into the rates of ordering near T_c. However, due to the sluggishness of the LRO process, T_c cannot be accurately determined. Moreover the energy released during ordering cannot be accurately measured.

From dynamic tests quantitative results can be obtained, when the experimental conditions are carefully controlled (low heating rate, adjustment of the base line, choice of the limits for the peak-area measurements). The change in enthalpy between different states of order may be measured. For example the transition from the LRO state at 150 °C to the SRO state at 300 °C is accompanied by an enthalpy change of 1060 J $(g\ at)^{-1}$. A good agreement is found by a Monte-Carlo method [28] using α parameters measured by X-ray diffuse scattering [1030 J $(g\ at)^{-1}$].

The change in the equilibrium value of the LRO parameter S vs. temperature can be followed from the enthalpy changes on disordering pre-annealed samples. The curve does not present any discontinuity at T_c. This behaviour is therefore quite different from the theoretical one. Values of S decrease rapidly with increasing temperature, with the variation nearly linear just below T_c. This trend suggests the existence of a two-phase region of ordered and disordered phases.

LRO kinetics can be obtained. The LRO kinetics of $Au_{75}Cu_{25}$ and $Au_{70}Cu_{30}$ proceed through a two-stage process: first a rapid one, due both to the establishment of SRO and to the nucleation of LRO, and secondly a very slow one due to the development of LRO.

SRO kinetics can be obtained. The SRO rate is clearly faster for $Au_{70}Cu_{30}$ than for $Au_{75}Cu_{25}$. The energy changes involved are smaller than those we have measured for changes in chemical order on studying the enthalpy relaxation of amorphous metallic alloys [2,4,5].

REFERENCES

1 H.S. Chen, in T. Masumoto and K. Suzuki (Eds.), Proc. 4th Intern. Conf. on Rapidly Quenched Metals. The Japan Inst. of Metals, Sendai, 1982, Vol. I, p. 495.

2 M. Harmelin, Y. Calvayrac, A. Quivy, J. Bigot, P. Burnier and M. Fayard, J. Non-Cryst. Solids, 61/62 (1984) 931.
3 E. Balanzat and J. Hillairet, J. Phys. F, 12 (1982) 2907.
4 M. Harmelin, A. Sadoc, A. Naudon, A. Quivy and Y. Calvayrac, J. Non-Cryst. Solids, 74 (1985) 107.
5 S. Lefebvre, M. Harmelin, A. Quivy, J. Bigot, Y. Calvayrac and R. Bellissent, Intern. Conf. on Liquid and Amorphous Metals, 24–29 August, 1986, Garmish-Partenkirchen, F.R.G. (in press).
6 P. Tissot and D. Dallenbach,. Thermochim. Acta, 25 (1978) 143.
7 B. Batterman, J. Appl. Phys., 28 (1957) 556.
8 D. Gratias, M. Condat and M. Fayard, Phys. Status Solidi A, 14 (1972) 123.
9 D. Gratias, Thèse 3ème Cycle, Paris VI, 16 novembre 1972.
10 P.M. Bronsveld and S. Radelaar, J. Phys. Soc. Jpn, 38 (1975) 1336.
11 A. Van den Beukel, A.P. Matthijsen, J.M. Ritzen and R. den Buurman, Acta Metall., 16 (1968) 435.
12 B.M. Korevaar, Physica, 25 (1959) 1021.
13 B.M. Korevaar, Acta Metall., 8 (1961) 297.
14 M. Hirabayashi and Y. Muto, Acta Metall., 9 (1961) 497.
15 K. Van der Lee and A. Van den Beukel, Scripta Metall., 5 (1971) 901.
16 M. Hirabayashi, J. Phys. Soc. Jpn, 14 (1959) 262.
17 S. Radelaar and J.M. Ritzen, Phys. Status Solidi, 31 (1969) 277.
18 G.R. Platerink, Phil. Mag., 17 (1968) 327.
19 M. Bessière, S. Lefebvre and Y. Calvayrac, Acta Crystallogr. Sect B, 39 (1983) 145.
20 M. Bessière, Thèse, Paris VI, 1984.
21 M. Bessière, Y. Calvayrac, S. Lefebvre, D. Gratias and P. Cénédèse, J. Phys. Paris, 47 (1986) 1961.
22 G. Bessenay, Thèse, Paris VI, 1986.
23 F.M. d'Heurle and P. Gordon, Acta Metall., 9 (1961) 304.
24 J.L. Deneuville, D. Gratias, C. Chatillon-Colinet and J.C. Mathieu, C.R. Acad. Sci. Paris, Série C, 284 (1977) 776.
25 R.G. Davies and A.J. Funes, Acta Metall., 9 (1961) 978.
26 W.L. Bragg and E.J. Williams, Proc. R. Soc. London, Ser. A, 145 (1934) 699 and 151 (1935) 540.
27 J.J. Kessis, C.R. Acad. Sci. Paris, 270 (1970) 1.
28 F. Livet and M. Bessière, submitted to J. Phys. Paris.
29 Z.W. Wilchinsky, J. Appl. Phys., 15 (1944) 806.
30 B.W. Roberts, Acta Metall., 2 (1954) 597.
31 G. Renaud, M. Belakhovsky, J. Hillairet, M. Wuttig, G. Bessenay and S. Lefebvre, to be published in the Proc. of the Intern. Conf. on Internal Friction and Ultrasonic Attenuation in Solids. 23–28 July 1987, Antwerp, Belgium.
32 J.M. Cowley, Phys. Rev., 77 (1950) 669.